Communication: The description of strong correlation within self-consistent Green's function second-order perturbation theory

Jordan J. Phillips, and Dominika Zgid

Citation: The Journal of Chemical Physics **140**, 241101 (2014); doi: 10.1063/1.4884951
View online: https://doi.org/10.1063/1.4884951
View Table of Contents: http://aip.scitation.org/toc/jcp/140/24
Published by the American Institute of Physics

Articles you may be interested in

Self-consistent second-order Green's function perturbation theory for periodic systems
The Journal of Chemical Physics **144**, 054106 (2016); 10.1063/1.4940900

Communication: Towards ab initio self-energy embedding theory in quantum chemistry
The Journal of Chemical Physics **143**, 241102 (2015); 10.1063/1.4938562

Dynamical mean-field theory from a quantum chemical perspective
The Journal of Chemical Physics **134**, 094115 (2011); 10.1063/1.3556707

A comparison between the Mo/ller–Plesset and Green's function perturbative approaches to the calculation of the correlation energy in the many-electron problem
The Journal of Chemical Physics **93**, 5826 (1990); 10.1063/1.459578

Incremental full configuration interaction
The Journal of Chemical Physics **146**, 104102 (2017); 10.1063/1.4977727

One-particle many-body Green's function theory: Algebraic recursive definitions, linked-diagram theorem, irreducible-diagram theorem, and general-order algorithms
The Journal of Chemical Physics **147**, 044108 (2017); 10.1063/1.4994837

Communication: The description of strong correlation within self-consistent Green's function second-order perturbation theory

Jordan J. Phillips[a] and Dominika Zgid
Department of Chemistry, University of Michigan, Ann Arbor, Michigan 48109, USA

(Received 12 May 2014; accepted 12 June 2014; published online 25 June 2014)

We report an implementation of self-consistent Green's function many-body theory within a second-order approximation (GF2) for application with molecular systems. This is done by iterative solution of the Dyson equation expressed in matrix form in an atomic orbital basis, where the Green's function and self-energy are built on the imaginary frequency and imaginary time domain, respectively, and fast Fourier transform is used to efficiently transform these quantities as needed. We apply this method to several archetypical examples of strong correlation, such as a H_{32} finite lattice that displays a highly multireference electronic ground state even at equilibrium lattice spacing. In all cases, GF2 gives a physically meaningful description of the metal to insulator transition in these systems, without resorting to spin-symmetry breaking. Our results show that self-consistent Green's function many-body theory offers a viable route to describing strong correlations while remaining within a computationally tractable single-particle formalism. © *2014 AIP Publishing LLC*. [http://dx.doi.org/10.1063/1.4884951]

I. INTRODUCTION

The description of strong correlations arising from, for example, open shell d orbitals in transition metal complexes,[1,2] or degenerate π orbitals in polyaromatic organic compounds,[3] remains a significant challenge in quantum chemistry for several reasons. For example, while single-reference methods such as Kohn-Sham (KS) density functional theory[4] (DFT) can be cost-effective enough to apply to realistic systems, they flounder when confronted with multireference configurations that require a rigorous treatment of static correlation.[5,6] On the other hand, multireference methods that can handle these strong correlations, such as the complete (Refs. 7, 8) and restricted (Refs. 9, 10) active space self-consistent field methods, or the more recently developed multiconfigurational hybrid DFT schemes,[11–13] all share the same fundamental requirement of defining an active-space within which the number of determinants grows exponentially with the number of correlated orbitals. These challenges have motivated the exploration of alternate approaches for strongly correlated systems, such as the density matrix renormalization group (DMRG),[2,14–16] the two-electron reduced density matrix method,[3,17,18] constrained-pairing mean-field theory (CPMFT),[19–21] and projected Hartree-Fock theory (PHF).[22–27] Despite these developments, an inexpensive and generally applicable *ab initio* method that can simultaneously handle dynamic and strong static correlation remains elusive.

Green's function many-body theory[28] offers an interesting formalism to attack this problem. In various realizations such as GW,[29] the random phase approximation (RPA),[30,31] the nth-order algebraic diagrammatic construction (ADC(n)),[32] and second-order Green's function theory (GF2),[33] many-body theory has a long history of use for calculating properties such as ionization potentials and electron affinities, excited states, spectra, and ground-state properties as well.[34–39] While typically these methods have been applied to weakly correlated systems, it has long been known that they can work with varying degrees of success for simple multireference systems. For example, GW,[40–43] RPA,[5,44–50] and GF2[33,51] can give a qualitatively correct description of stretched H_2 without breaking spin-symmetry. Similarly, the ADC(n) method has been shown to accurately describe the spectra and excited states of multireference polyenes[52] and carbon clusters,[53] and recently in the Nuclear Physics community second-order Gorkov-Green's function theory[54,55] has found use for open shell nuclei featuring degeneracies.[56]

In this Communication, it is our purpose to show that GF2 can, without breaking spin-symmetry, give a qualitatively correct description of even nontrivial strongly correlated systems such as stretched H_{12} and H_{32} lattices, which are multireference even at their respective equilibrium lattice spacings. We will show that in terms of calculated energies, GF2 is similar to MP2 (Møller–Plesset second order) when the system is single-reference, yet more closely resembles truncated CI in the strongly correlated dissociation limit. Furthermore, at self-consistency GF2 yields fractional natural occupation numbers that can describe the metal-to-insulator transition in these lattices. This makes GF2 a viable formalism for systems too large for active-space methods, yet too strongly correlated for single-reference approaches, and offers a way to simply and efficiently extend MP2's treatment of dynamic correlation to strongly correlated systems while remaining within a tractable single-reference formalism.

First, we give an overview of the theory and our implementation of GF2. We stress that previous implementations of GF2-type methods by Holleboom and Snijders[33] as well as Dahlen and van Leeuwen[51] existed, however to the best of

[a]Author to whom correspondence should be addressed. Electronic mail: philljj@umich.edu

 © 2014 AIP Publishing LLC

our knowledge none of them investigated in detail the potential of GF2 to describe highly multireference systems, or an efficient implementation that can be useful by a more general community of computational chemists.

II. IMPLEMENTATION

In the following, we work in a non-orthogonal atomic orbital (AO) basis with corresponding overlap matrix **S**, Fock matrix **F**, and density matrix **P**. Starting from a restricted Hartree-Fock (HF) reference solution, in the AO basis the frequency dependent HF Green's function is built as $\mathbf{G}_{\mathrm{HF}}(\omega) = [(\mu + \omega)\mathbf{S} - \mathbf{F}]^{-1}$, where μ is the chemical potential, ω is an imaginary frequency, and **F** is given by $F_{ij} = h_{ij} + \sum_{kl} P_{kl}(\mathrm{v}_{ijlk} - \frac{1}{2}\mathrm{v}_{iklj})$, where h_{ij} are matrix elements of one electron operators and v_{ijkl} are two-electron integrals in the AO basis.

Provided with $\mathbf{G}_{\mathrm{HF}}$, the exact single-particle many-body Green's function, $\mathbf{G}(\omega)$, can be found by solving the Dyson equation $\mathbf{G}(\omega) = \mathbf{G}_{\mathrm{HF}}(\omega) + \mathbf{G}_{\mathrm{HF}}(\omega)\Sigma(\omega)\mathbf{G}(\omega)$, where $\Sigma(\omega)$ is the exact frequency-dependent self-energy which accounts for the correlation missing in the simple HF picture. In this work, we employ a second-order approximation to the self-energy, which is shown using Feynman diagrams[57] in Figure 1. Starting from the left the first two are the first-order Hartree and exchange diagrams. This is the frequency independent part of the self-energy, and is already covered by the Fock matrix **F**. The next two diagrams are second-order, and are given algebraically in the time domain as

$$\Sigma_{ij}(\tau) = -\sum_{klmnpq} G_{kl}(\tau)G_{mn}(\tau)G_{pq}(-\tau) \times \mathrm{v}_{imqk}(2\mathrm{v}_{lpnj} - \mathrm{v}_{nplj}), \quad (1)$$

where $\mathbf{G}(\tau)$ is the Green's function Fourier transformed to the imaginary time domain. With the self-energy constructed, we can fast Fourier transform (FFT) $\Sigma(\tau)$ to the ω domain and build the Green's function as

$$\mathbf{G}(\omega) = [(\mu + \omega)\mathbf{S} - \mathbf{F} - \Sigma(\omega)]^{-1}. \quad (2)$$

Provided with an updated Green's function, we can build the correlated single-particle density matrix **P** (see Eq. (5) in the supplementary material[58]) and then build the correlated Fock matrix **F**. Equations (1) and (2) therefore establish a self-consistent scheme for calculating the Green's function in a second-order approximation. The detailed description of the implementation steps can be found in Sec. I of the supplementary material.[58] To evaluate the GF2 electronic energy, we employ the Galitskii–Migdal formula[59] (see Sec. II of the supplementary material[58]).

Let us now discuss several advantages of the GF2 theory that may make it accessible and interesting for a general quantum chemistry community. GF2 is an iterative procedure where the central quantity of interest is the single-particle many body Green's function $\mathbf{G}(\omega)$, rather than the single-particle density $\rho(\mathbf{r})$ or the many-body wavefunction Ψ. In the GF2 scheme, there is no explicit reference to Ψ, thus the requirement of choosing an active-space or truncating Ψ at a certain excitation level is circumvented entirely. This offers an enormous reduction in computational effort for systems that require large active-spaces, and gives GF2 generous flexibility in handling systems that would require different levels of excitations in a CI expansion (e.g., singles, doubles, triples, etc.). Additionally, unlike KS-DFT, which depends explicitly on a $\rho(\mathbf{r})$ built from a non-interacting reference of Kohn-Sham orbitals obeying Aufbau filling, GF2 has no problem confronting strongly correlated systems and can yield fractional natural occupation numbers at self-consistency. Furthermore, because of its iterative self-consistent nature GF2 is independent of the reference Green's function, and thus both HF and DFT starting Green's functions can be used. In the final solution, series of diagrams are included due to the inexplicit resummation in the iterative procedure. This is the reason why GF2 is able to recover some static correlation even when starting from a restricted-HF solution, and can avoid the typical MP2 divergence for cases with decreasing band gaps. Moreover, due to the inclusion of series of mosaic diagrams this method is applicable to metallic systems[60,61] when the regular MP2 method would remain pathologically divergent.

The building of $\Sigma(\tau)$ according to Eq. (1) formally scales as $O(N_\tau n^5)$, where N_τ and n are the number of imaginary time grid points and atomic orbitals, respectively. While N_τ presents a significant prefactor, at any given grid point τ_n the construction of the self-energy Σ_{τ_n} is independent, and therefore as a whole the self-energy formation is embarrassingly parallel. Given the development in technology in the last few decades, it is not unreasonable to have access to a computing facility offering several hundred to tens of thousands of processors for parallel computing. Therefore, practically speaking, the formal scaling of $O(N_\tau n^5)$ will never be realized in typical calculations, and the reality will be much closer to $O(n^5)$.

Since the self-energy in Eq. (1) can be expressed in the imaginary time domain as a product of the Green's functions with the two-electron integrals, the whole GF2 calculation can be performed in the AO basis. Thus, the costly orbital

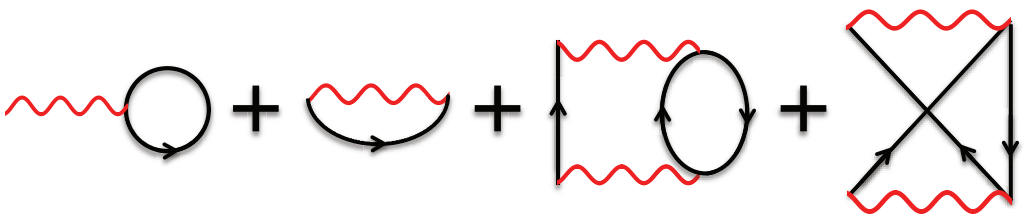

FIG. 1. Diagrams included in second-order self-energy within GF2. The first two diagrams are frequency-independent, and are included in the Fock matrix. The next two diagrams are frequency-dependent, and represent the second-order correlation effects covered by $\Sigma(\omega)$.

transformations from AO to molecular orbital (MO) basis are not necessary, and one can take advantage of integral screening which should reduce the computation cost even further. This is due to a similar structure of the second order self-energy in the time domain to the Laplace transformed MP2 expressions. An alternative route leading to a significant cost reduction is using density fitted AO integrals in Eq. (1), which would result in $O(n^3m)$ scaling where the m is the number of auxiliary functions necessary for density fitting. Thus, as expected the overall scaling of the GF2 algorithm is identical up to a prefactor with the Laplace transformed density fitted MP2 scheme.

To build $\Sigma(\tau)$, we employ a non-equidistant τ grid with a sufficient number of points for the Fourier transforms to be converged to a very high precision.[62] We use FFT that scale as $O(N\log(N))$, where N is the number of grid-points. High accuracy in the FFT integrals is maintained since we use an analytical high frequency tail of the Green's function,[63,64] given by $\mathbf{G}(\omega) \approx \frac{\mathbf{G}_1}{\omega} + \frac{\mathbf{G}_2}{\omega^2} + \frac{\mathbf{G}_3}{\omega^3}$. To build $\mathbf{G}(\omega)$, we use a grid of Matsubara frequencies, $\omega_n = (2n + 1)i\pi/\beta$. Imaginary frequencies are used in our implementation because $\mathbf{G}(\omega)$ is a smoother function on the imaginary axis as compared to the real axis, which simplifies its numerical evaluation significantly. We find it useful to choose the inverse temperature β and number of frequency points such that the initial Hartree-Fock Green's function reproduces the Hartree-Fock energy and electron number to 10^{-5} precision. This brings us to the next advantage of the GF2 method, which is the inverse temperature β makes the GF2 calculation explicitly temperature dependent.[65] All other computationally demanding steps of the GF2 algorithm such as constructing the Green's function and evaluation of the chemical potential scale as $O(n^3)$ and are cheaper than the construction of $\Sigma(\tau)$.

We emphasize that this GF2 procedure is all-electron, with no selection of an active space of correlated orbitals. Other than the choice of an appropriate frequency/time grid (which usually is straightforward), the GF2 procedure requires no more user input than that of a typical HF or DFT calculation. As such it can be made blackbox.

III. RESULTS AND DISCUSSION

Now we report the application of our GF2 implementation for several representative cases of strong correlation. We want to stress that all GF2 calculations are spin-restricted, and are compared to other spin-restricted calculations using standard *ab initio* methods (e.g., RHF, MP2, configuration interaction singles doubles (CISD), coupled cluster singles doubles (CCSD), etc.). The DALTON 2011 suite of programs[66] was used to carry out all calculations, as well as to generate the restricted Hartree-Fock input required for our in-house GF2 implementation.

Before we discuss the dissociation curves, it is worth making a very brief remark on the relevance of self-interaction error (SIE), which can manifest in many-body theory[67–69] and DFT.[70] Because SIE can "mimic" static correlation,[69,71] its presence (absence) can actually appreciably improve (worsen) the performance of a method in the dissociation limit.[47,48] Because GF2 includes all direct and exchange diagrams up to second order it is therefore explicitly SIE-free, in contrast to other many-body methods such as GW or RPA.[68,69] Therefore, the static correlation GF2 recovered in our calculations is the result of a genuine treatment of correlation rather than a fortuitous exploitation of SIE errors.

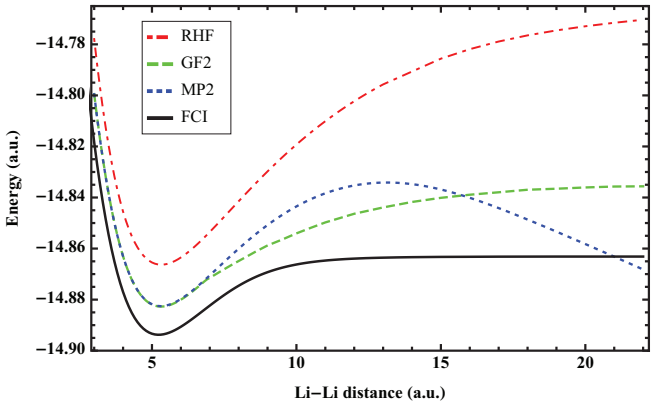

FIG. 2. Dissociation of Li_2 with 6-31G basis.

First, we consider the Li_2 dissociation with the 6-31G basis, shown in Figure 2. For this system, we compare RHF, MP2, and full configuration interaction (FCI) to GF2. The natural occupation numbers obtained with GF2 for this system (as well as the other systems studied in this work) can be found in Sec. III of the supplementary material.[58] Interestingly, MP2 and GF2 are practically identical within the equilibrium distance and up to about 7 a.u. Beyond 7 a.u. the MP2 and GF2 curves separate, and the GF2 solution transitions from weakly to strongly correlated. MP2, unable to cope with the multireference character of the strongly correlated solution, characteristically begins to diverge to $-\infty$ correlation energy with infinite separation while GF2 converges to a finite value parallel to FCI.

Next, we consider the H_6 ring stretch using a TZ basis, which is shown in Figure 3. Due to the high multireference character in the dissociation limit both CCSD and coupled cluster singles doubles with perturbative triples (CCSD(T)) fail spectacularly. MP2 and GF2 are in very close agreement around the equilibrium distance where the system is still essentially single-reference. Beyond $a = 3.5$ a.u. the system rapidly takes on multi-reference character and the GF2 curve

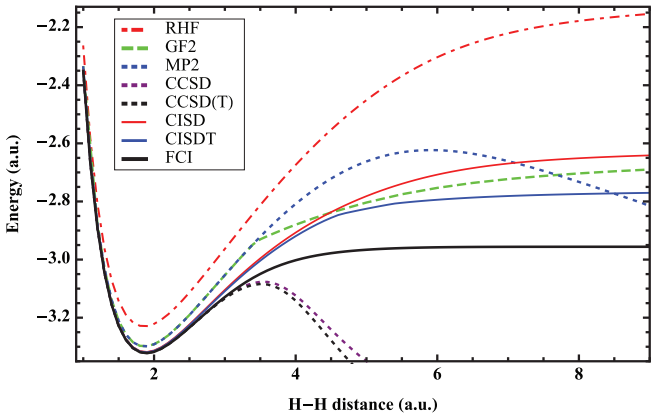

FIG. 3. Dissociation of H_6 with TZ basis.

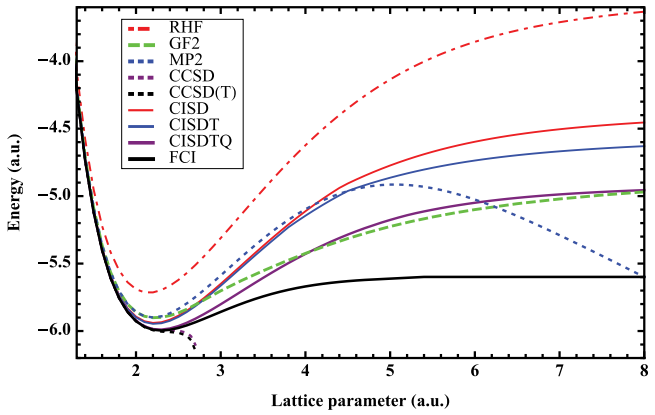

FIG. 4. Dissociation of H_{12} with STO-3G basis.

breaks away from MP2, which coincides with the divergence of CCSD and CCSD(T) away from the FCI curve. In the dissociation limit, GF2 settles out between the CISD and CISDT curves.

Now we apply GF2 to two finite hydrogen lattices, a 4×3 hydrogen plaquette (H_{12}) and a 4×4×2 hydrogen lattice (H_{32}). The structures of both systems are determined by the lattice parameter a. Hydrogen chains and lattices are an interesting test case because they can display highly multireference electronic ground states at stretched lattice parameters, and accounting for the metal-to-insulator transition with changing lattice parameter is a challenging test for an *ab initio* method.[15,18,72]

First, we consider the 4×3 hydrogen plaquette with a minimal STO-3G basis (Fig. 4). This system is interesting as it displays strong correlations even at the equilibrium lattice spacing. Because of this MP2 and GF2 begin to separate from each other near the bottom of the well around 2.3 a.u., while CCSD and CCSD(T) cannot even qualitatively describe the equilibrium energy curve. In this case in the dissociation limit, GF2 gives an energy very similar to CISDTQ. Excepting of course FCI, of all the methods considered *only* GF2 was able to capture the physically correct limit with all 12 natural occupation numbers approaching unity in the dissociation limit.

Finally, we consider the H_{32} finite cubic lattice, which is even more strongly correlated within the equilibrium lattice spacing than H_{12}. In Figure 5, we plot the natural occupation numbers of the correlated density-matrix as obtained by GF2 with respect to the lattice parameter a. Additionally, in the lower-right inset we show the lattice structure, and in the upper-right inset we show dissociation curves for RHF, MP2, CISD, and GF2. We attempted coupled cluster calculations on this system but could not converge for $a \geq 2.0$ a.u., similar to Hachmann, Cardoen, and Chan's[15] experience with the H_{50} chain. Examining first the natural occupation numbers, for $a < 2.0$ a.u. the system is approximately single-reference, but it is visible the GF2 natural occupations are smoothly shifting towards stronger correlations. By $a \approx 2.0$ a.u. a weakly to strongly correlated transition has occurred, and for $a \geq 2.0$ a.u. the system smoothly becomes more strongly correlated, with all 32 natural occupation numbers approaching unity in the limit of large lattice parameter a. This shows that GF2 can capture the metal-to-insulator

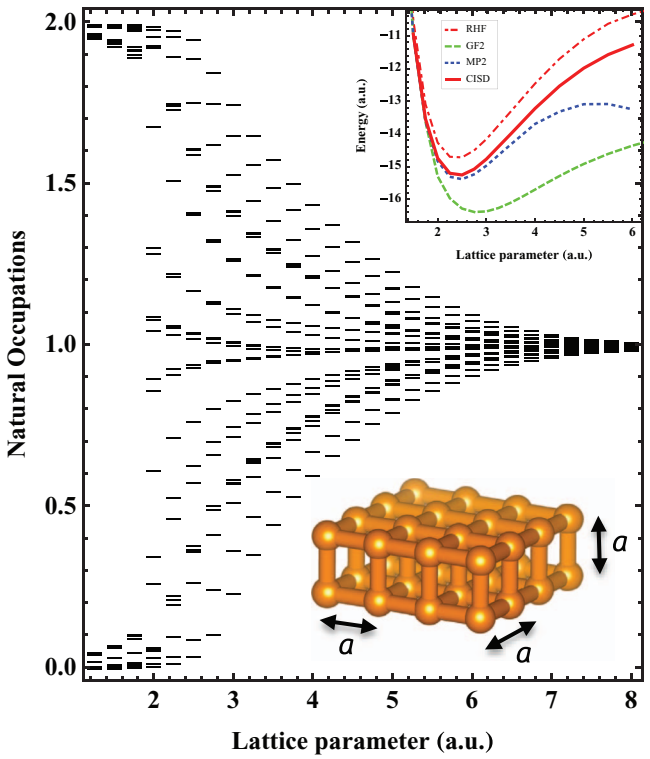

FIG. 5. Natural occupation numbers of H_{32} double plaquette with respect to lattice parameter a. Inset lower-right: structure of H_{32} (image generated by VESTA[73]). Inset upper-right: lattice stretching curves for RHF (dotted-dashed red), MP2 (dotted blue), CISD (thick red), and GF2 (dashed green).

transition in a strongly correlated system while being essentially a single-reference-type blackbox method.

Inspecting the lattice-stretching curve in the upper-right inset now, we see that already by $a = 2.0$ a.u. the MP2 and GF2 curves have separated, because of the strong correlations present near the equilibrium lattice spacing. Interestingly, the CISD curve is slightly worse than MP2, which indicates the truncated CI expansion of Ψ would need to include much higher excitations than merely doubles, which is consistent with the natural occupation numbers from GF2.

In conclusion, GF2 is an all-electron, size-extensive, *ab initio* blackbox method that due to iterative diagrammatic resummation can recover both dynamic and static correlation. This allows it to avoid the typical collapse inherent to the MP2 method when strong correlations are present, and furthermore enables GF2 to describe phenomena such as the metal-to-insulator transition in strongly correlated electronic systems. Additionally, GF2 gives immediate access to temperature dependent properties, and is a good formalism for calculating frequency dependent quantities as well. Moreover, GF2 can be trivially implemented in a massively parallel fashion, and it can scale as $O(n^3m)$ with density fitted integrals, thus making it affordable. Further work is necessary to provide additional validation of GF2's performance for more realistic systems, but even in its current form this method can be used to help determine the active space orbital choice or provide a starting point for procedures such as dynamical mean field theory (DMFT).[74,75] Due to its low computational scaling, blackbox nature, ability to recover multireference character and AO-based implementation, GF2 also makes an ideal can-

didate for extension to periodic systems. One can also dare to conjecture, based on some earlier results with selective CC resummation for the electron gas,[61] that a periodic GF2 implementation would be applicable to both metals and insulators.

ACKNOWLEDGMENTS

D. Zgid and J. J. Phillips acknowledge support from a (U.S.) Department of Energy (DOE) Grant No. ER16391 and an XSEDE allocation allowing us to use the STAMPEDE supercomputer.

[1] I. de P. R. Moreira and F. Illas, Phys. Chem. Chem. Phys. **8**, 1645 (2006).
[2] K. H. Marti and M. Reiher, Phys. Chem. Chem. Phys. **13**, 6750 (2011).
[3] K. Pelzer, L. Greenman, G. Gidofalvi, and D. A. Mazziotti, J. Phys. Chem. A **115**, 5632 (2011).
[4] R. G. Parr and W. Yang, *Density-Functional Theory of Atoms and Molecules* (Oxford University Press, New York, 1989).
[5] M. Fuchs, Y.-M. Niquet, X. Gonze, and K. Burke, J. Chem. Phys. **122**, 094116 (2005).
[6] A. J. Cohen, P. Mori-Sánchez, and W. Yang, Chem. Rev. **112**, 289 (2012).
[7] B. O. Roos, P. R. Taylor, and P. E. Siegbahn, Chem. Phys. **48**, 157 (1980); P. Siegbahn, A. Heiberg, B. Roos, and B. Levy, Phys. Scr. **21**, 323 (1980); P. E. M. Siegbahn, J. Almlöf, A. Heiberg, and B. O. Roos, J. Chem. Phys. **74**, 2384 (1981).
[8] K. Andersson, P. A. Malmqvist, B. O. Roos, A. J. Sadlej, and K. Wolinski, J. Phys. Chem. **94**, 5483 (1990); K. Andersson, P. A. Malmqvist, and B. O. Roos, J. Chem. Phys. **96**, 1218 (1992).
[9] J. Olsen, B. O. Roos, P. Jorgensen, and H. J. A. Jensen, J. Chem. Phys. **89**, 2185 (1988).
[10] P. A. ke Malmqvist, K. Pierloot, A. R. M. Shahi, C. J. Cramer, and L. Gagliardi, J. Chem. Phys. **128**, 204109 (2008).
[11] T. Leininger, H. Stoll, H. Werner, and A. Savin, Chem. Phys. Lett. **275**, 151 (1997).
[12] E. Fromager, J. Toulouse, and H. J. A. Jensen, J. Chem. Phys. **126**, 074111 (2007).
[13] K. Sharkas, A. Savin, H. J. A. Jensen, and J. Toulouse, J. Chem. Phys. **137**, 044104 (2012).
[14] U. Schollwöck, Rev. Mod. Phys. **77**, 259 (2005).
[15] J. Hachmann, W. Cardoen, and G. K.-L. Chan, J. Chem. Phys. **125**, 144101 (2006).
[16] G. K.-L. Chan and D. Zgid, Annu. Rep. Comput. Chem. **5**, 149 (2009).
[17] G. Gidofalvi and D. A. Mazziotti, J. Chem. Phys. **129**, 134108 (2008).
[18] A. V. Sinitskiy, L. Greenman, and D. A. Mazziotti, J. Chem. Phys. **133**, 014104 (2010).
[19] V. N. Staroverov and G. E. Scuseria, J. Chem. Phys. **117**, 11107 (2002).
[20] T. Tsuchimochi and G. E. Scuseria, J. Chem. Phys. **131**, 121102 (2009).
[21] G. E. Scuseria and T. Tsuchimochi, J. Chem. Phys. **131**, 164119 (2009).
[22] C. A. Jiménez-Hoyos, T. M. Henderson, T. Tsuchimochi, and G. E. Scuseria, J. Chem. Phys. **136**, 164109 (2012).
[23] A. J. Garza, C. A. Jiménez-Hoyos, and G. E. Scuseria, J. Chem. Phys. **138**, 134102 (2013).
[24] P. Rivero, C. A. Jiménez-Hoyos, and G. E. Scuseria, J. Phys. Chem. A **117**, 8073 (2013).
[25] P. Rivero, C. A. Jiménez-Hoyos, and G. E. Scuseria, J. Phys. Chem. B **117**, 12750 (2013).
[26] T. Stein, C. A. Jiménez-Hoyos, and G. E. Scuseria, J. Phys. Chem. A (published online).
[27] L. Bytautas, C. A. Jiménez-Hoyos, R. Rodrguez-Guzmn, and G. E. Scuseria, Mol. Phys. (published online).
[28] A. Fetter and J. Walecka, *Quantum Theory of Many-particle Systems*, Dover Books on Physics (Dover Publications, 2003).
[29] L. Hedin, Phys. Rev. **139**, A796 (1965).
[30] D. Bohm and D. Pines, Phys. Rev. **82**, 625 (1951); D. Pines and D. Bohm, *ibid.* **85**, 338 (1952); D. Bohm and D. Pines, *ibid.* **92**, 609 (1953).
[31] M. Gell-Mann and K. A. Brueckner, Phys. Rev. **106**, 364 (1957).
[32] J. Schirmer, Phys. Rev. A **26**, 2395 (1982); J. Schirmer, L. S. Cederbaum, and O. Walter, *ibid.* **28**, 1237 (1983); A. Tarantelli and L. S. Cederbaum, *ibid.* **39**, 1656 (1989).
[33] L. J. Holleboom and J. G. Snijders, J. Chem. Phys. **93**, 5826 (1990).
[34] J. D. Doll and W. P. Reinhardt, J. Chem. Phys. **57**, 1169 (1972).
[35] P. Langhoff and A. Hernandez, Chem. Phys. Lett. **49**, 361 (1977).
[36] M. Jaszunski, B. Pickup, and R. McWeeny, Chem. Phys. Lett. **90**, 167 (1982).
[37] L. S. Cederbaum, Int. J. Quantum Chem. **38**, 393 (1990).
[38] J. Cioslowski and J. V. Ortiz, J. Chem. Phys. **96**, 8379 (1992).
[39] J. V. Ortiz, WIREs: Comput. Mol. Sci. **3**, 123 (2013).
[40] A. Stan, N. E. Dahlen, and R. van Leeuwen, EPL **76**, 298 (2006).
[41] N. E. Dahlen, R. van Leeuwen, and U. von Barth, Phys. Rev. A **73**, 012511 (2006).
[42] A. Stan, N. E. Dahlen, and R. van Leeuwen, J. Chem. Phys. **130**, 114105 (2009).
[43] F. Caruso, P. Rinke, X. Ren, A. Rubio, and M. Scheffler, Phys. Rev. B **88**, 075105 (2013).
[44] F. Furche, Phys. Rev. B **64**, 195120 (2001).
[45] F. Aryasetiawan, T. Miyake, and K. Terakura, Phys. Rev. Lett. **88**, 166401 (2002).
[46] M. Fuchs, K. Burke, Y.-M. Niquet, and X. Gonze, Phys. Rev. Lett. **90**, 189701 (2003).
[47] J. E. Bates and F. Furche, J. Chem. Phys. **139**, 171103 (2013).
[48] F. Caruso, D. R. Rohr, M. Hellgren, X. Ren, P. Rinke, A. Rubio, and M. Scheffler, Phys. Rev. Lett. **110**, 146403 (2013).
[49] J. E. Moussa, J. Chem. Phys. **140**, 014107 (2014).
[50] T. Olsen and K. S. Thygesen, J. Chem. Phys. **140**, 164116 (2014).
[51] N. E. Dahlen and R. van Leeuwen, J. Chem. Phys. **122**, 164102 (2005).
[52] J. H. Starcke, M. Wormit, J. Schirmer, and A. Dreuw, Chem. Phys. **329**, 39 (2006); *Electron Correlation and Multimode Dynamics in Molecules* (in honour of Lorenz S. Cederbaum).
[53] M. S. Deleuze, M. G. Giuffreda, J.-P. Franois, and L. S. Cederbaum, J. Chem. Phys. **111**, 5851 (1999).
[54] L. Gorkov, Sov. Phys.-JETP **7**, 505 (1958).
[55] V. Somà, T. Duguet, and C. Barbieri, Phys. Rev. C **84**, 064317 (2011); V. Somà, C. Barbieri, and T. Duguet, *ibid.* **89**, 024323 (2014).
[56] V. Somà, C. Barbieri, and T. Duguet, Phys. Rev. C **87**, 011303 (2013).
[57] R. Mattuck, *A Guide to Feynman Diagrams in the Many-body Problem*, Dover Books on Physics Series (Dover Publications, Inc., 1976).
[58] See supplementary material at http://dx.doi.org/10.1063/1.4884951 for a detailed description of our GF2 implementation, as well as plots of natural occupation numbers for these systems.
[59] V. Galitskii and A. Migdal, Sov. Phys. JETP **7**, 96 (1958).
[60] We based this conclusion on the work of Scuseria where inclusion of mosaic diagrams prevented divergence of perturbative scheme for electron gas. Since mosaic diagrams are included in GF2 resummation, we conclude that such method must work for periodic metallic systems.
[61] J. J. Shepherd, T. M. Henderson, and G. E. Scuseria, J. Chem. Phys. **140**, 124102 (2014); Phys. Rev. Lett. **112**, 133002 (2014).
[62] A. Albuquerque, F. Alet, P. Corboz, P. Dayal, A. Feiguin, S. Fuchs, L. Gamper, E. Gull, S. Gürtler, A. Honecker, R. Igarashi, M. Körner, A. Kozhevnikov, A. Läuchli, S. Manmana, M. Matsumoto, I. McCulloch, F. Michel, R. Noack, G. Pawłowski, L. Pollet, T. Pruschke, U. Schollwöck, S. Todo, S. Trebst, M. Troyer, P. Werner, and S. Wessel, J. Magn. Magn. Mater. **310**, 1187 (2007), in Proceedings of the 17th International Conference on Magnetism.
[63] A. B. Comănac, "Dynamical mean field theory of correlated electron systems: New algorithms and applications to local observables," Ph.D. thesis, Columbia University, 2007.
[64] E. Gull, "Continuous-time quantum Monte Carlo algorithms for fermions," Ph.D. thesis, ETH Zürich, 2008.
[65] The number of τ grid points depends on the inverse temperature β and the number of frequency points. In our calculations, we use a very high value of $\beta = 200 - 300$ in order to mimic zero-temperature calculations. In such cases, we commonly employ 4000τ grid points. For lower values of the inverse temperature β, it is possible to use around $100 - 400\tau$ grid points and achieve a high accuracy.
[66] K. Aidas, C. Angeli, K. L. Bak, V. Bakken, R. Bast, L. Boman, O. Christiansen, R. Cimiraglia, S. Coriani, P. Dahle, E. K. Dalskov, U. Ekström, T. Enevoldsen, J. J. Eriksen, P. Ettenhuber, B. Fernández, L. Ferrighi, H. Fliegl, L. Frediani, K. Hald, A. Halkier, C. Hättig, H. Heiberg, T. Helgaker, A. C. Hennum, H. Hettema, E. Hjertenæs, S. Høst, I.-M. Høyvik, M. F. Iozzi, B. Jansík, H. J. A. Jensen, D. Jonsson, P. Jørgensen, J. Kauczor, S. Kirpekar, T. Kjærgaard, W. Klopper, S. Knecht, R. Kobayashi, H. Koch, J. Kongsted, A. Krapp, K. Kristensen, A. Ligabue, O. B. Lutnæs, J. I. Melo, K. V. Mikkelsen, R. H. Myhre, C. Neiss, C. B. Nielsen, P. Norman, J. Olsen, J. M. H. Olsen, A. Osted, M. J. Packer, F. Pawlowski, T. B. Pedersen, P. F. Provasi, S. Reine, Z. Rinkevicius, T. A. Ruden, K. Ruud, V. V. Rybkin, P. Sałek, C. C. M. Samson, A. S. de Merás, T. Saue, S. P. A. Sauer,

B. Schimmelpfennig, K. Sneskov, A. H. Steindal, K. O. Sylvester-Hvid, P. R. Taylor, A. M. Teale, E. I. Tellgren, D. P. Tew, A. J. Thorvaldsen, L. Thøgersen, O. Vahtras, M. A. Watson, D. J. D. Wilson, M. Ziolkowski, and H. Gren, WIREs: Comput. Mol. Sci. **4**, 269 (2014).
[67]M. E. Casida and D. P. Chong, Phys. Rev. A **44**, 5773 (1991).
[68]W. Nelson, P. Bokes, P. Rinke, and R. W. Godby, Phys. Rev. A **75**, 032505 (2007).
[69]T. M. Henderson and G. E. Scuseria, Mol. Phys. **108**, 2511 (2010).
[70]J. P. Perdew and A. Zunger, Phys. Rev. B **23**, 5048 (1981).
[71]V. Polo, E. Kraka, and D. Cremer, Mol. Phys. **100**, 1771 (2002).
[72]L. Stella, C. Attaccalite, S. Sorella, and A. Rubio, Phys. Rev. B **84**, 245117 (2011).
[73]K. Momma and F. Izumi, J. Appl. Crystallogr. **41**, 653 (2008).
[74]A. Georges, G. Kotliar, W. Krauth, and M. J. Rozenberg, Rev. Mod. Phys. **68**, 13 (1996).
[75]D. Zgid and G. K.-L. Chan, J. Chem. Phys. **134**, 094115 (2011).